Available online at www.sciencedirect.com
ScienceDirect
Journal of the European Ceramic Society 31 (2011) 2809–2817
www.elsevier.com/locate/jeurceramsoc

Comparison of micropatterning methods for ceramic surfaces

Marzellus Grosse Holthaus, Laura Treccani, Kurosch Rezwan *

University of Bremen, Advanced Ceramics, Am Biologischen Garten 2, 28359 Bremen, Germany

Received 5 May 2011; received in revised form 6 July 2011; accepted 21 July 2011
Available online 15 August 2011

Abstract

The fabrication of defined ceramic micropatterns smaller than 100 μm is due to the hardness and brittleness of ceramic materials still very challenging. However, in recent years, micropatterned ceramic surfaces have become highly interesting for biomedical applications or the fabrication of energy converting devices, such as solid oxide fuel or solar cells. In this study we evaluate six modern techniques for ceramic pattern fabrication with feature sizes ranging from 5 to 100 μm. Ceramic materials such as alumina, zirconia, silica and hydroxyapatite are discussed. Advantages and disadvantages for each process are highlighted and compared to the other techniques. Three of these techniques, namely microtransfer molding, modified micromolding and Aerosol-Jet® printing generate patterns starting with aqueous ceramic suspensions. The other three techniques, micromachining and two different types of laser treatment produce micropatterns by material removal from solid ceramic substrates. The detailed analysis yields that properties such as the desired micropatterning size, shape or the production time are strongly dependant on the chosen technique.

Keywords: Micropatterning; Ceramic; Molding; Machining; Laser treatment; Aerosol jet printing

1. Introduction

Micropatterned surfaces are gaining ongoing interest in the field of materials research and industrial manufacture. They have become state of the art and opened new fields of potential applications for the fabrication of e.g. micromolds with modulated microtopographies[1] or for the modification of micro-bio-interfaces to guide interactions between cell tissue and medical implant surfaces.[2,3] The development and improvement of surface micro- and nanopatterning was in the focus of materials research for the last 20 years. Thereby, various techniques for the fabrication of patterned surfaces have been developed. These techniques were reviewed by a large number of research groups.[4–8]

Ceramic materials are of great interest for micropatterning processes, because they exhibit advantageous properties compared to polymers and metals such as high thermal resistance, chemical inertness, high hardness and biocompatibility. However, obtaining ceramic micropatterns with high accuracy, e.g. precise edge contours, is very challenging due to the particular hardness and typically brittle behaviour of ceramic materials. For the surface patterning of ceramic materials mainly two different strategies can be applied. First of all there is the possibility of machine-aided ceramic micropatterning with a high effort of technical equipment. Examples are laser surface treatment, injection molding of microparts, slip pressing or casting of microdevices and micromachining of surfaces by e.g. CNC-machining (Computer Numerical Control). Beyond doubt, the results of the machine-aided methods are convincing. Bauer et al. reported the reliable fabrication of microparts with high accurate edge contours and surface details by the use of ceramic slip pressing. Thereby, alumina arrays of more than a thousand columns have been fabricated with smooth sidewalls and sharp edges. The fabricated patterns were 455 μm high and 115 μm wide.[9] Other groups reported reproducible results from the fabrication of microdevices via ceramic injection molding (CIM), in particular with low pressure injection molding (LPIM) of ceramic feedstocks. Various ceramic materials such as alumina, hydroxyapatite and zirconia have been used to reliably produce micropatterned components of a few cm^2 in size.[10–12] Some of these machine-aided processes yielded remarkable results in terms of micropattern edge contours and process reliability. One main advantage is the potential fabrication of a high number of items per time. The limiting factor however is the difficulty in obtaining micropatterns or components smaller

* Corresponding author. Tel.: +49 421 218 4507; fax: +49 421 218 7404.
E-mail addresses: mgrh@uni-bremen.de (M.G. Holthaus), treccani@uni-bremen.de (L. Treccani), krezwan@uni-bremen.de (K. Rezwan).

0955-2219/$ – see front matter © 2011 Elsevier Ltd. All rights reserved.
doi:10.1016/j.jeurceramsoc.2011.07.020

than 100 μm. A different approach to fabricate highly defined ceramic patterns is the possibility of using low cost methods such as soft-lithography techniques.[8] Soft-lithography is capable to fabricate micropatterns with a low technical effort and very high accuracy – even smaller than 100 μm – at the same time.

This study evaluates the results of six different micropatterning techniques for ceramic materials for obtaining structural features beneath 100 μm. Non-oxide ceramic hydroxyapatite and at least one oxide material such as alumina or zirconia were used as material to be patterned. The following techniques are evaluated: Microtransfer molding (μTM), modified micromolding (m-μM), Aerosol-Jet® printing, CNC-micromachining and two types of laser treatment. Each technique was tested and evaluated for ceramic micropatterning size features ranging from 5 to 100 μm.

2. Experimental procedures

Six different processing techniques were applied to fabricate micropatterned ceramic surfaces. For CNC-micromachining and two types of laser treatment solid ceramic substrates were used. From these samples material was removed to form micropatterned surfaces. For the other three techniques, namely microtransfer molding, modified micromolding and Aerosol-Jet® printing, the micropatterns were obtained by starting with aqueous ceramic suspensions.

2.1. Fabrication of non-patterned substrates

Plane cylindrical, non-patterned platelets were fabricated by uniaxially die-pressing with 15 kN of 1.7 g commercially available calcium phosphate hydroxyapatite powder (HA, $Ca_{10}(PO_4)_6(OH)_2$, Prod.-No. 04238, Lot: 8345A, Sigma–Aldrich Chemie GmbH, Munich, Germany). The HA powder had a theoretical density of 3.03 ± 0.04 g/cm^3 and particle sizes of 151 ± 0.24 nm. After die-pressing all samples were sintered for 2 h at 1200 °C in a furnace at ambient conditions (LHT08/17, Nabertherm GmbH, Lilienthal, Germany). The heating rate was 50 °C/h, the cooling rate at 100 °C/h. Except for modified micromolding, the non-patterned samples were used for all patterning processes.

2.2. Fabrication of aqueous ceramic suspensions for molding and printing

Three different ceramic suspensions were used for the patterning processes. One suspension contained 11.15 g of HA particles. The HA powder was stirred (RW20, IKA Werke GmbH, Staufen, Germany) into 20 g of double deionised water (Synergy®, Millipore, resistivity 18 MΩ cm, Schwalbach, Germany) to obtain a suspension of 15 vol.% solid loading. The ceramic suspension was adjusted to pH 9–10 by the addition of ammonia solution (25%) to achieve electrostatic stability and to prevent agglomeration of the particles. This ceramic suspension was used as a stamping liquid for the microtransfer molding (μTM) process. Another ceramic suspension was used as a ceramic "ink" for Aerosol-Jet® printing processes. It was similar to the first suspension, but it was diluted to a solid loading of 6.6 vol.%. The third suspension was used for modified micromolding. Its composition was similar to the one used for liquid stamping, but additionally a polyacrylic acid-based dispersant/binder was added (12 mg/g ceramic powder). Prior to micropatterning all ceramic suspensions were homogenised using ultrasonic treatment (Sonifier 450, Branson Ultraschall, Dietzenbach, Germany) for 3 min to disperse potential agglomerates.

2.3. Micropatterning techniques

2.3.1. Microtransfer molding

For the microtransfer molding (μTM) process a ceramic suspension was pipetted onto the micropatterned area of a soft mold (PDMS, Sylgard® 184 silicone elastomer, Dow Corning, Wiesbaden, Germany). Excessive suspension was carefully removed with a doctor's blade. Subsequently, the filled mold was deposited on a plane ceramic substrate. After drying the mold was lifted with carefully. The patterned thin film remained on the substrate during the removal of the mold (Fig. 1a). Hereafter the ceramic substrate and ceramic patterns were sintered. A more detailed description of this method can be found in Holthaus and Rezwan.[13] Generally, adjustable parameters for microtransfer molding are e.g. drying conditions, dispersants and binders, particle sizes and solid loadings of used ceramic suspensions.

2.3.2. Modified micromolding

Similar to the microtransfer molding process, micropatterned soft PDMS master molds were used for modified micromolding (m-μM). The cylindrical molds were sealed with polyethylene tubes and aqueous ceramic suspension was pipetted into the molding chamber. During the drying process the ceramic particles sink to the bottom of the mold, while water is continuously evaporating. After drying the mold could be lifted with care from the micropatterned solid ceramic sample. Afterwards sintering was performed as mentioned above. Additional details about this method are described by Holthaus et al.[14] (Fig. 1b). Adjustable parameters for modified micromolding are e.g. drying conditions, binders and dispersants, solid loading of the ceramic suspensions and particle size.

2.3.3. Aerosol-Jet® printing

Aerosol-Jet® printing (Optomec Inc., Albuquerque, USA), also known as maskless mesocale materials deposition (M^{3}D), was used for the direct printing of ceramic aerosols on non-patterned ceramic substrates. The aerosol of a ceramic suspension was generated with an ultrasonic transducer. The printing device is computer-aided and was used to deposit the ceramic particles on specific positions onto the plane substrate. The particles were carried by a gas and deposited by a nozzle onto the substrate. Subsequent sintering of the printed microstructures by a NdYAG-laser (Newport Spectra-Physics, Darmstadt, Germany) was proceeded. Further information about this experiment is provided in Holthaus and Rezwan[13] (Fig. 1c). Adjustable parameters for Aerosol-Jet® printing are related to the used ceramic suspensions e.g. dispersants

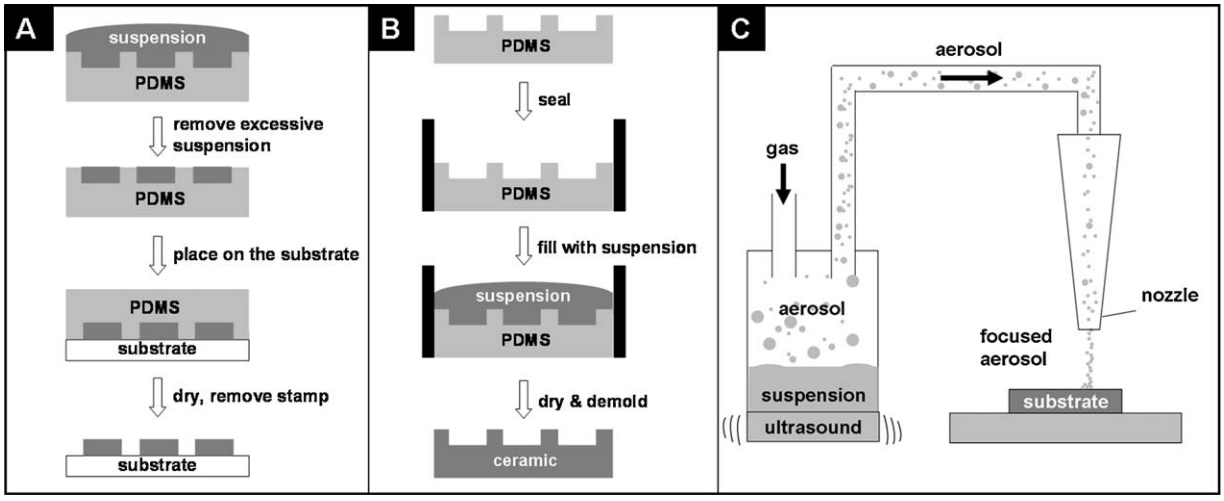

Fig. 1. Illustrations of micropatterning techniques using aqueous ceramic suspension. A: microtransfer molding (μTM). B: modified micromolding (m-μM). C: Aerosol-Jet® printing (M^3D).

and binders, particle sizes and solid loading. Additionally, process parameters such as the feed motion of the print head, the distance between nozzle and substrate, the repetition of printing cycles on identical locations and the power of the laser are important parameters for the patterning result.

2.3.4. CNC-micromachining

Automated CNC-milling and -grinding (Ultrasonic 20 linear, DMG Sauer GmbH, Stipshausen, Germany) was applied on solid ceramic substrates. During the cutting process the workpiece was held stationary as the rotating cutting tool moved along a programmed path to cut the material. Machining was operated with so called end milling cutters, namely ball-nose end mills. The tools cut using their sides as well as their tips, whereas the contact force during machining removed particles from the surface layer of the ceramic substrate (Fig. 2a). Generally, the rotational speed (n), the feed velocity (vf) and the diameter of the cutting tool (D) are important adjustable parameters influencing the machining results.

2.3.5. Laser treatment

Two different laser treatment processes were applied. By the use of the first laser treatment ceramic particles were directly removed from the solid ceramic substrate by thermal laser ablation at ambient conditions via a Nd:YAG laser (Newport Spectra-Physics) at a wavelength of 1064 nm. Thereby ceramic particles were removed by the laser beam from a flux zone in the irradiated area (Fig. 2b). A more detailed description of this treatment is given in Holthaus and Rezwan.[13]

The second laser treatment technique was direct laser interference patterning (DLIP). In this procedure, the laser provides a fundamental wavelength of 1064 nm (Nd:YAG, Newport Spectra-Physics). An applied wavelength of 266 nm was obtained by harmonic generation via a shutter. The laser beam was split into two coherent laser beams which interfered on the ceramic substrate surface. This interference process produced micropatterns on the irradiated area of several square millimetres (Fig. 2c). Further details of this method can be found in Berger et al.[15] Various parameters such as the laser power, the laser beam wavelength, the number of laser pulses or the pulse duration are important parameters for the adjustment of both laser treatment processes.

2.4. Imaging of surface texture and analysis of surface roughness

Micrographs were taken at 20 kV by a scanning electron microscopy (SEM) with a Camscan Series 2 (Obducat

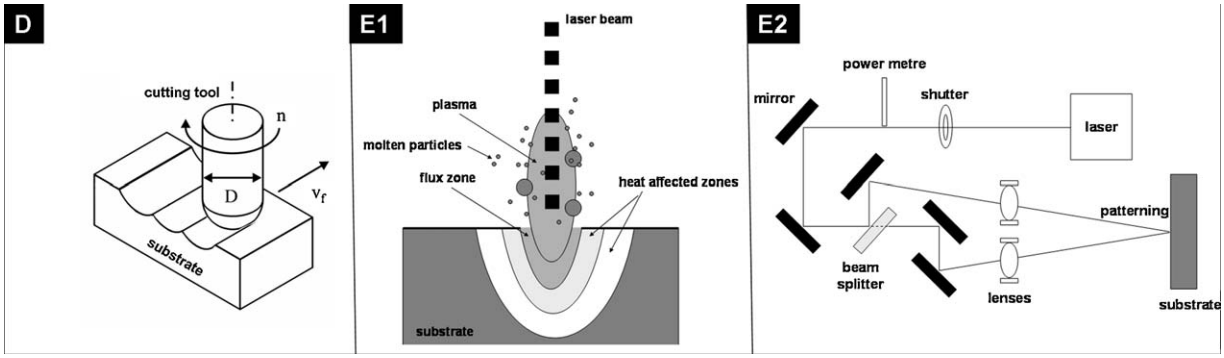

Fig. 2. Illustrations of different micropatterning techniques. D: CNC-micromachining via a cutting tool of tool diameter (D), rotational speed (n) and feed velocity (vf). E1: laser ablation process. E2: set-up of direct laser interference patterning (DLIP).

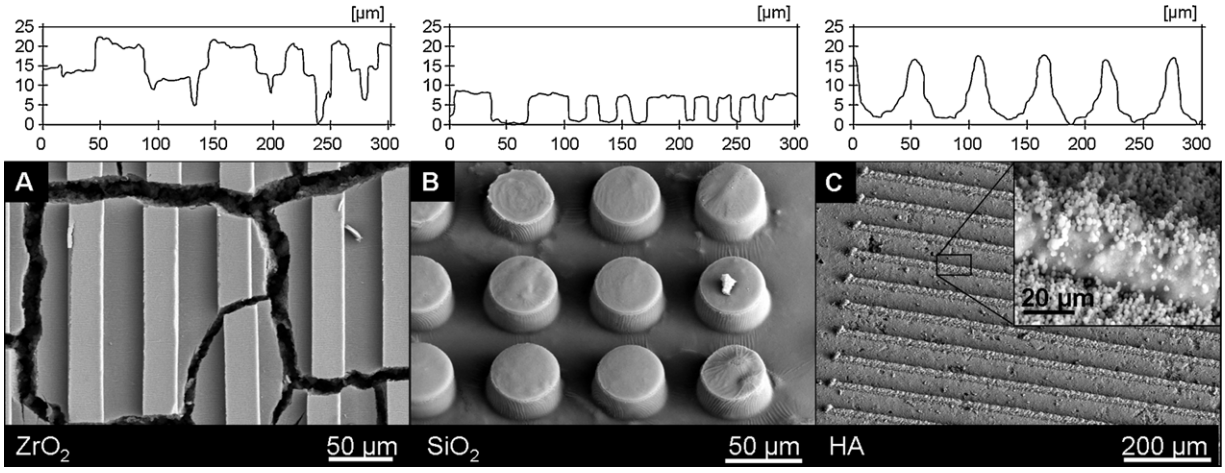

Fig. 3. SEM micrographs of micropatterned ceramic surfaces. A: microtransfer molded 30 µm wide zirconia channels, B: modified micromolded 50 µm wide SiO_2 cylinders, C: Aerosol-Jet®-printed 10 µm wide HA struts. Inset shows magnification of a printed and sintered line. 2D-profiles show representable profiles of fabricated ceramic patterns.

CamScan Ltd., Cambridgeshire, United Kingdom). Prior to imaging the samples were sputtered with gold (K550, Emitech, Judges Scientific plc, West Sussex, United Kingdom).

3D-measurements of fabricated ceramic micropatterns were taken via a confocal optical profilometry system (Plµ 2300, Sensofar Technology, Terrassa, Spain) at 420-fold magnification. Measurements in triplicate have been conducted on $n = 3$ samples each. Within the profilometry analysis the average surface roughness (Ra) of micropatterned areas was determined. The measurement length was $L_c = 4$ mm according to ISO4287 (ISO 4287, 1997). These measurements were applied to evaluate the influence of each micropatterning process on the surface roughness in the patterning region. In addition virtual cross-sections (2D-surface profiles) were exemplary measured for one sample of each micropatterning method.

2.5. Determination of crystal structure and analysis of surface properties

Samples of all applied patterning methods were analysed via X-ray diffraction measurements (XRD, C3000, Seifert, Ahrensburg, Germany) to determine possible changes in crystal structure due to the patterning technique.

Two methods were used to detect possible wear residues from e.g. tools from the patterning process. Firstly, energy dispersive spectroscopy (EDS, Camscan Series 2, Obducat CamScan Ltd., Cambridgeshire, United Kingdom) with a detection limit of about 0.1% of the elements mass was used. Two different spots with an area of $27 \times 17\ \mu m^2$ each were measured. Secondly, X-ray fluorescence analysis (XRF) was conducted to detect residues from the patterning process (detection limit of approximately 10 ppm). XRF measurement was carried out using a low and a high pass filter (0–40 keV, XL3t900 AnalytiCON Instruments GmbH, Rosbach, v.d. Hoehe, Germany). Measurements were taken on two different circular spots with an area of 7.1 mm^2 each. Prior to the EDS and XRF analysis the samples were washed three times for 5 min in deionised water in an ultrasonic cleaner.

3. Results

3.1. Micropatterned ceramic thin films stamped via microtransfer molding (µTM)

The drying of microtransfer molded ceramic surfaces took about 2–3 days at ambient conditions (~21 °C, 30–40% r.h.) and up to 6 days at 4 °C. Although it was possible to fabricate ceramic samples without any cracks after the drying process, all samples showed very fine micron sized cracks after sintering. The cracks occurred on the whole sample surface. However, accurate micropatterns with vertical sidewalls were clearly visible. Various pattern geometries such as microcylinders and – channels and – struts have been successfully transfer molded. Although excessive ceramic suspension was removed from the mold, a layer of suspension below the patterns was always transferred to the substrate surface. The thickness of the transferred thin films varied between 20 and 110 µm. The accuracy in height of single transferred patterns was homogenous after drying (±1 µm). The smallest transferred HA patterns were 10 µm in width featuring heights of 10 µm. All patterned areas looked craggy and fissured after sintering, whereas microchannels and microstruts were still accurate and had defined contour on edges. Due to big cracks the accuracy of patterns height was strongly reduced (±4 µm) after sintering. The accuracy of sintered patterns varied ±2 µm in width. The average surface roughness inside sintered transfer molded HA microchannels was Ra = 2.9 µm.

The microtransfer molded ZrO_2 patterns shown in Fig. 3(A) were fabricated using a suspension of 15 vol.%. The patterns dried at ambient conditions. XRD analysis of transfer molded and sintered HA samples showed no detectable changes in crystal structure e.g. peaks of β-tricalcium phosphate (β-TCP). Other ceramic suspensions such as alumina have been transfer molded with similar results.

3.2. Micropatterned solid ceramic bodies fabricated via modified micromolding (m-μM)

Solid micropatterned ceramic samples were fabricated via modified micromolding and dried for up to 5 days at ambient conditions. The drying period could be decreased to 2 days by using a climate chamber at 30 °C and 30% r.h. The crack-free fabrication of patterned solid ceramic samples was feasible with various ceramic suspensions. Thereby different geometries such as cylinders, struts, and microchannels with widths and depths ranging from 5 to 200 μm have been successfully fabricated. The molded micropatterns featured very accurate edge contours after drying and sintering. Molded patterns measured on different samples varied ±1.4 μm in height and ±1.2 μm in width after sintering.

The molded patterns shown in Fig. 3(B) were fabricated using a SiO_2 suspension of 10 vol.% with 12 mg Syntran®/g ceramic. The samples dried at 25 °C with 25% r.h. and were sintered at 1400 °C. The average roughness inside and outside patterned areas was identical. For example a roughness of Ra = 0.2 μm was measured inside sintered molded HA patterns. XRD analysis of a modified micromolded and sintered HA samples showed no changes in crystal structure.

3.3. Aerosol-Jet® printed ceramic micropatterns on ceramic substrates

The complete Aerosol-Jet®-patterning of a ceramic sample as shown in Fig. 3(C) needed roughly 3 h. The printed micropatterns showed a grainy surface and did not feature vertical sidewalls and accurate edge contours. Single ceramic particles or agglomerates were visible on top of the fabricated patterns as well as next to the patterned regions. The Aerosol-Jet®-printed patterns dried within seconds, thus a controlled drying process was not applicable. Various pattern geometries such as circles and lines have been successfully printed. After the laser-treatment the ceramic particles were not fully sintered and showed partially only sinter neck formation. A few fine cracks were distinguished within the generated structures. The sintering quality varied strongly. Some regions of the micropatterns were more sintered than others and some were already molten. The micropattern size was limited by the size of a single printed line. The smallest adjustable printed lines were ranging between 10 and 15 μm in width and height. The heights of printed micropatterns on different samples varied between ±4 μm and ±3 μm in width. It was possible to print multi-layers to fabricate e.g. micropatterns with widths of 50 μm and heights of almost 30 μm. The average roughness on aerosol printed regions was Ra = 4.1 μm. The focused aerosol beam had to be re-adjusted often, due to an inconstant aerosol flow.

The patterns shown in Fig. 3(C) were fabricated by printing single lines of HA suspension (6.6 vol.%) using a feed motion of the printer nozzle at 0.5 mm/s. Afterwards the patterns were sintered using a Nd:YAG laser (1064 nm) with a power of 0.25 W. The lateral laser movement was at 0.5 mm/s. XRD analysis of a laser sintered aerosol printed HA sample showed no changes in crystal structure.

3.4. CNC-micromachined solid ceramic samples

By using grinding pins or milling tools in the micromachining process it was possible to fabricate large ceramic micropatterns of several cm^2. The complete machining of each ceramic sample needed roughly 60 min. In both cases periodic groove-like micropatterns were machined. In addition, other pattern geometries such as pyramid-like patterns have been successfully machined in preliminary tests. Milled HA samples exhibited U- and V-shaped topographies and their surface was chipped and rough. In contrast, grinding delivered sharply edged grooves (rectangle profile) with pattern sidewalls almost vertical and perpendicular to the bottom area. Microgrinding resulted in smoother surface roughness as compared to milling. However, the surface roughness of all CNC-machined regions was ranging from Ra = 0.3 to 0.8 μm. The smallest machined patterns were 100 μm in width with a maximum pattern depth of about 10 μm. Smaller patterns of 75 μm in width were achieved by re-sintering micromachined ceramic green bodies due to shrinkage. Comparing identically machined samples, the accuracy in pattern width was ±3 μm and ±2 μm in depth. The ZrO_2 micropatterns in Fig. 4D were machined using a ball-end grinding pin with a tool diameter of 500 μm, a feed velocity of 125 mm/min, and a rotational speed of 40.000 rpm. XRD analysis of machined HA samples showed no alterations in crystal structure. Although strong defects due to abrasive wear were found on the machine tools, no residues from the tools were detectable via XRF analysis or EDS after three washing processes in double deionised water using an ultrasound cleaner.

3.5. Laser treated ceramic surfaces

The ablation process of a ceramic sample took about ~10 min. The fabricated microchannels showed U-/V-shaped profiles. The surface of these ablated patterns looked rough and bumpy. Thereby the surface of microchannels with widths of 40 μm and 80 μm seemed to be partially molten. The surface of microchannels with widths of 220 μm looked molten as well, but also rough and craggy. The contour of ablated pattern edges was inaccurate and rough. The surface roughness inside microchannels of 220 μm in width was Ra = 14.8 μm. Rough surfaces with drop-shaped bumps were noticed next to laser ablated regions e.g. on the struts between the channels. It seemed like molten ceramic particles solidified there subsequently after ablation. The depth of the laser ablated micropatterns varied between 30 and 110 μm, whereas the depth increased by increasing channel width. The accuracy in pattern height was ±10 μm. The accuracy in pattern width was ±8 μm. The adjustment of laser power, to get constant ablation quality, was difficult. Furthermore it was not feasible to generate smaller micropatterns than ~30 μm on die-pressed ceramic substrates without a significant loss of micropattern edge contour. The HA micropatterns shown in Fig. 4(E1) were laser ablated using a Nd:YAG laser with a wavelength of 1064 nm with a pulse duration of 100 ns. The laser power was 3.5 W and a feed motion of 16 mm/s was used. XRD analysis of laser ablated HA samples showed no change of crystal structure, but amorphous fractions due to the massive

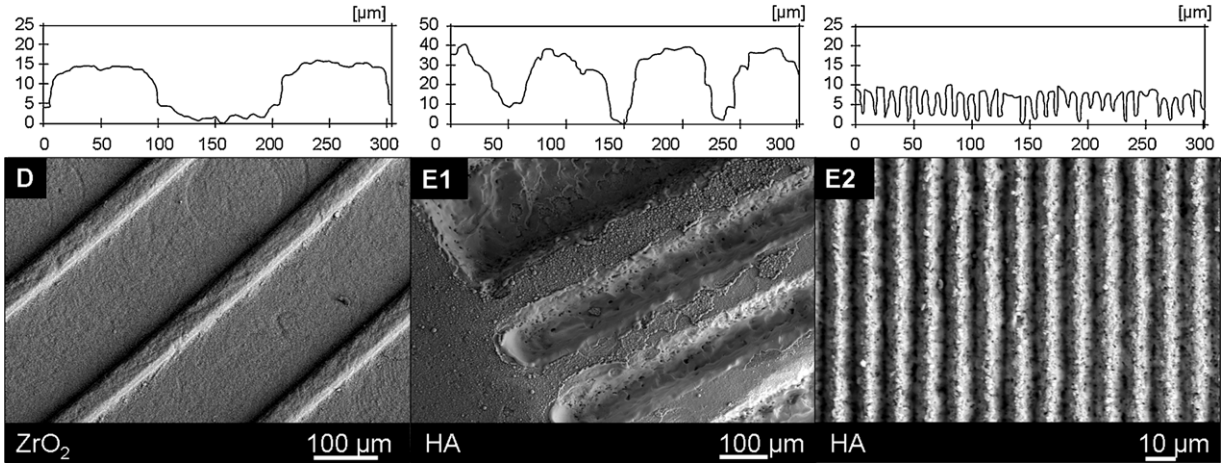

Fig. 4. SEM micrographs of micropatterned ceramic surfaces. D: micromachined (grinding) 200 µm wide ZrO_2 channels, E1: laser ablated HA microchannels with widths of 40 µm (centre), E2: laser interference patterned 10 µm wide HA channels. 2D-profiles show representable profiles of fabricated ceramic patterns.

heat impact are most likely. The oxide ceramic alumina was patterned in initial testings (Fig. 5E1).

Direct laser interference patterning (DLIP) conducted on plane ceramic surfaces resulted in periodic patterns with U-/V-shaped pattern profiles. The effects of laser fluence, periodic distance, pulse number and wavelength were investigated, whereas it was found that there is a range of laser fluences and pulse numbers where homogenous ceramic patterns can be developed. Different interference patterns such as line- and cross-like arrays were fabricated using single laser pulse or multi laser pulses. The generation of large area patterning with distinct patterns of several mm^2 was applicable by using only one single laser pulse. The patterning of total sample surfaces took about a few minutes. The interference patterns showed a distinct geometry, but their surfaces looked rough and partially molten. The contour on pattern edges was inaccurate and rough. The measured surface roughness inside patterns was $Ra = 2.1$ µm. Smallest producible line-like patterns were 10 µm in width. Pattern depths ranging from 0.5 µm to 6 µm have been fabricated controllably. The accuracy of pattern width as well as pattern depth was ± 1 µm when comparing different samples.

The HA patterns shown in Fig. 4(E2) were generated using a wavelength of 266 nm, a laser fluence of 0.6 J/cm^2 and 50 pulses with durations of 10 ns each. Other materials such as oxide ceramics alumina and zirconia were patterned in initial testings (Fig. 5E2). No significant changes were detectable by XPS analysis of untreated and DLIP-treated HA substrates with a laser fluence of 4.8 J/cm^2 and 10 laser pulses.

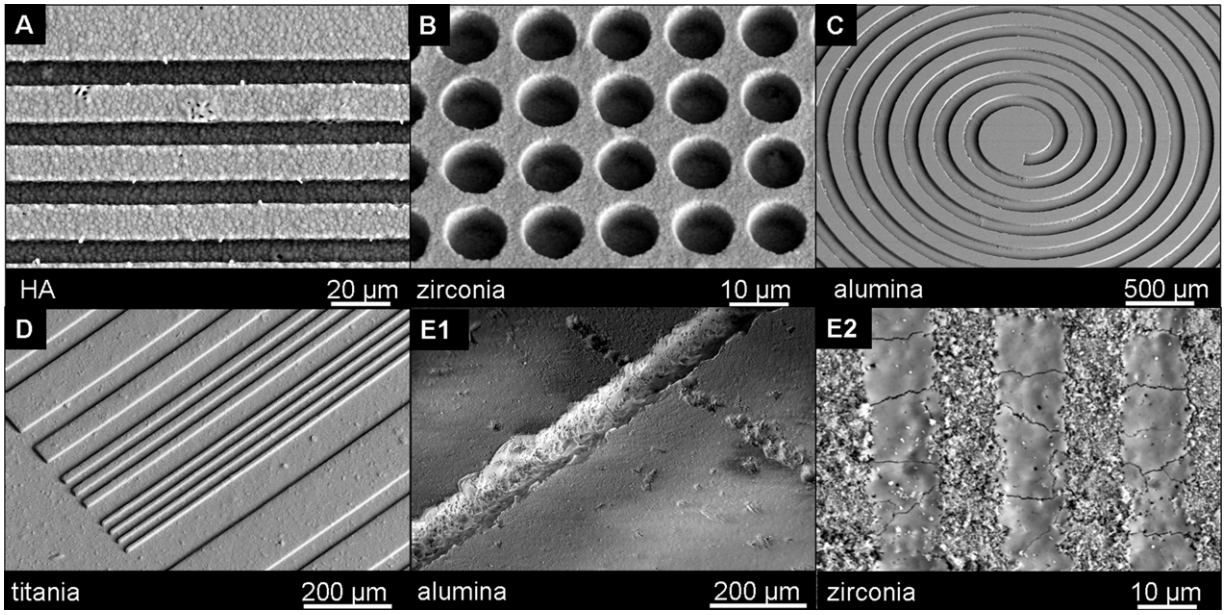

Fig. 5. Micromolded ceramics (A–D) and laser treated ceramic surfaces (E). A: sintered (1200 °C) hydroxyapatite microchannels with widths of 8 µm. B: sintered (1500 °C) zirconia holes with diameters of 8 µm. C: alumina spiral with channel widths of 100 µm. D: Titania microstruts with varying widths between 10 and 140 µm. E1: microchannel on laser ablated pre-sintered (1000 °C) alumina surface. E2: pre-sintered (1100 °C) laser interference patterned zirconia surface with line-like patterns of 10 µm in width.

4. Discussion

Microtransfer molding was used to fabricate micropatterned thin films with various pattern geometries as small as 10 μm with very high accuracy on edge contour. Even suspensions containing e.g. fluorescently labelled biomolecules such as protein BSA (bovine serum albumin) have been successfully patterned to ceramic surfaces and glass slides (data not shown). The deviations of ±4 μm in pattern height and ±2 μm in width on different ceramic transfer-patterned samples were promising. Disadvantageous is the production time of some days due to the drying process. One advantage is the low cost for equipment. The occurrence of cracks is strongly dependant on processing parameters such as the substrate surface, the sintering process or the amount of stamped material. The lower the amount of stamped material, the lower the presence of cracks. The maximum success rate for crack-free drying on glass slides was about 70%, whereas the maximum crack-free drying on a ceramic (HA) surface was only 15%. All sintered samples showed cracks. However, until the occurrence of cracks is not fully avoided, the μTM process is not applicable for large area patterning of ceramics surfaces.

It was possible to fabricate micropatterned solid ceramic samples via modified micromolding. Various materials and geometries have been successfully used (Fig. 5A–D). The smallest fabricated patterns were only 5 μm in width and height, whereas the edge contour was still very high. Smaller patterns have not been fabricated with any other tested technique. The deviations of molded patterns on different samples were ±1 μm in height and width. One big disadvantage is the long production time of a few days. Advantageous of m-μM is the joint processing of the substrate/device and the micropatterns at once. The success rates for crack-free drying with subsequent sintering were different for the used ceramic materials and strongly dependant on process parameters. However, success rates of 88% were reached for HA and even 100% for zirconia and alumina. The main advantage is the high output of crack-free ceramic micropatterns. Other advantages are low costs for the equipment and the possibility of the local deposition of molecules on patterned regions by the use of the μTM method. This was successfully tested with BSA on micromolded HA and alumina patterns with widths of 50 μm (data not shown). One property which differentiated m-μM from all other tested patterning techniques, was an identical surface roughness on patterned and non-patterned regions. Except for the etching of the master molds, no complex devices or machines are needed for this soft-lithographic-based technique, which makes this method accessible to a wide range of users.

Using Aerosol-Jet® printing it was feasible to generate patterns of 10 μm in width. The contour on edges and the achieved deviations of ±4 μm in pattern height and ±3 μm in width on different samples were not that high compared to m-μM. A big advantage is the possibility to print maskless patterns of various materials onto the same substrate. Even printing of different materials onto the same sample is feasible as well. Aerosol-Jet® printing is a useful automated fast processing method, whereas samples can be patterned within hours. Disadvantageous is the occurrence of molten areas in the patterning regions due to the uncontrollable sintering temperature by the adjustment of the laser power. Amorphous phases or change in crystal structure cannot be excluded. However, this is avoidable by sintering in a furnace at controlled conditions. Big disadvantage are high costs for the equipment.

Using CNC-micromachining the limit in pattern width was 100 μm, which was much larger when compared to all other techniques. Although smaller geometries of 75 μm in width could be realized by resintering, these patterns are still larger compared to other techniques. The shape of the machined ceramic patterns depended on the chosen machine tool, whereas U- and V-shaped as well as rectangular shaped pattern profiles have been successfully fabricated on oxide and non-oxide ceramic surfaces. The contour on pattern edges was high, but lower when compared to m-μM. The deviations of machined samples were ±2 μm in pattern depth, but were always minimum 12% lower than the predicted (calculated) pattern depth. Deviations of ±3 μm were achieved in pattern width on different samples. The surface roughness (Ra = 0.3–0.8) of machined regions was lower compared to other techniques such as laser treatment. Disadvantages are potential wear residues from cutting tools on the patterned surfaces, the size of the smallest producible patterns and high costs for equipment. Advantages are the automated and fast, maskless manufacture of solid patterned samples within hours.

The use of laser ablation resulted in patterns with a minimum width of 30 μm, tested on oxide and non-oxide ceramics. This is not as small as fabricated via m-μM or Aerosol-Jet® printing, but much smaller compared to micromachining. Ablated pattern edges looked inaccurate, whereas the pattern surface was either rough and craggy or molten. In molten regions amorphous phases or change in crystal structure cannot be excluded. The deviations between patterns of ablated samples were ±10 μm in height and ±8 μm in width. These values were the largest measured deviations of all tested techniques. The average roughness on ablated regions (Ra = 14.8 μm) was the highest Ra-value of all tested techniques. Another disadvantage is the high cost for equipment. However, laser ablation is a fast and maskless process for the fabrication of micropatterned solid ceramic samples.

Direct laser interference patterning resulted in various shaped micropatterns with minimum widths of only 10 μm on oxide and non-oxide ceramics. The accuracy on pattern edges was lower compared to m-μM, but much higher compared to common laser ablation. The deviations of interference patterned structures on different samples were ±1 μm in height and width, which was as low as using m-μM. The average roughness on DLIP-patterned regions (Ra = 2.1 μm) was similar as low as obtained by Aerosol-Jet® printing. Disadvantageous are high costs for equipment and regions with molten surfaces. Important advantages of DLIP are a maskless processing and the very fast patterning of large areas using only few laser pulses feasible.

Highly accurate microgeometries with vertical sidewalls generated via molding could be used e.g. for biological applications such as fluidic chambers, sensor surfaces or for fundamental cell-surface research or for novel types of energy conversion cells. Because of its possibility to print various materials into the same pattern, Aerosol-Jet® printing could be useful e.g. for

Table 1
Overview on properties of micropatterning techniques for ceramic materials.

Properties	Method					
	Stamping via microtransfer molding (μTM)	Modified micromolding (m-μM)	Aerosol-Jet® printing with laser sintering (M^3D)	Micro-machining via CNC	Laser ablation	Direct laser interference patterning (DLIP)
Smallest pattern size in *x*/*y*[a]	10 μm	5 μm	10 μm	100 μm	30 μm	10 μm
Are various pattern geometries producible?	Yes	Yes	Yes	Yes	Yes	Yes
Contour accuracy on edges	Very high	Very high	Middle	High	Middle	Middle
Surface roughness (Ra) of patterned regions[a]	∼3 μm	∼0.2 μm	∼4 μm	∼0.3–0.8 μm	∼15 μm	∼2 μm
Tolerances in height/depth (*z*)[a,b]	±4 μm	±1 μm	±4 μm	±2 μm (>12%)	±10 μm	±1 μm
Tolerances in width (*x*,*y*)[a]	±2 μm	±1 μm	±3 μm	±3 μm	±8 μm	±1 μm
Final product	μ-Patterned thin film on substrate	μ-Patterned solid ceramic sample	μ-Patterned thin film on substrate	μ-Patterned solid ceramic sample	μ-Patterned solid ceramic sample	μ-Patterned solid ceramic sample
Is joint processing of substrate & pattern possible?	No	Yes	No	No	No	No
Was a change of crystal structure detectable after patterning?	No	No	No	No	No. However localized amorphous phases very likely	No. However localized amorphous phases very likely
Possible contamination by residues from e.g. tools?	No	No	No	Yes	No	No
Is in situ deposition of other particles/biomolecules possible by this method?	Yes	Yes (via μTM)	Yes	No	No	No
Method applicable for oxide and non-oxide ceramics?	Yes	Yes	Yes	Yes	Yes	Yes
Production time from raw material to final product	Days	Days	Hours	Hours	Hours	Hours
Is sintering required after patterning?	Yes	Yes	Yes	No	No	No
Are masks/templates needed?	Yes	Yes	No	No	No	No
Is industrial upscaling possible?	Yes	Yes	Yes	Yes	Yes	Yes
Costs for equipment	Low	Low	High	High	High	High

[a] Measurements in triplicate of neighbouring patterns were taken on $n = 3$ final micropatterned products made of HA.
[b] Machined depths were minimum 12% lower than predicted pattern depths, which were calculated before machining.

applications where different materials have to be integrated into the same processing step such as layer-wise printing of conductive metallic paths and isolating ceramic parts for sensor applications. CNC-micromachining is applicable for the patterning of ceramic implant surfaces or even for the manufacture of whole ceramic implants with inline-processing of specific surface patterning to mediate the implant in-growth into the body. Laser treatment of ceramic surfaces could be applied to pattern ceramic implant surfaces too or to modulate surfaces of ceramic bearings to optimize friction and wear. In summary all tested patterning techniques are very useful to fabricate ceramic micropatterns smaller than 100 μm. The fabricated micropattern surfaces and geometries are different when comparing all methods, which enables a wide range of potential applications. An overview on the properties of each patterning technique is given in Table 1.

5. Conclusions

All tested patterning techniques are useful to fabricate ceramic micropatterns, but each tested process has its advantages and disadvantages compared to the other techniques. On the one hand general properties such as the costs for equipment are affecting the choice for a patterning technique. On the other hand the desired kind of micropattern geometry, accuracy, or size are also affected by this choice, which limits the number of suitable patterning methods in situations, for instance, in which a specific surface finish turns out indispensable. Micropatterns as small as 5 μm with vertical sidewalls can be achieved by modified micromolding. These patterns feature very high accuracy and low technical effort at the same time. But, the production time from the raw material to the final patterned product takes some days. A faster processing is Aerosol-Jet® printing, but the accuracy is lower and the costs for equipment are higher. Via micromachining it is not possible to fabricate ceramic patterns smaller than 100 μm and the costs for the equipment are high. Nevertheless it is a fast process for the patterning of various ceramic solid materials. Laser treatment processes have high costs for technical equipment, but the production time is low. Especially direct interference patterning offers a fast and accurate patterning of ceramic surfaces.

Acknowledgements

This work was financially supported by the University of Bremen (ZF-Kennz. 04/110/06). We thank Fraunhofer Institute for Material and Beam Technology Dresden for DLIP experiments, Laboratory for Precision Machining Bremen for the machining of samples, Institute for Microsensors, Actuators and Systems Bremen for etched master molds, Fraunhofer Institute for Manufacturing Technology and Advanced Materials Bremen for Aerosol-Jet® printing experiments and Bremer Institut für Angewandte Strahltechnik for laser ablated samples.

References

1. Brinksmeier E, Gläbe R, Riemer O, Twardy S. Potentials of precision machining processes for the manufacture of micro forming molds. *Microsyst Technol* 2008;**14**(12):1983–7.
2. Kirmizidis G, Birch MA. Microfabricated grooved substrates influence cell–cell communication and osteoblast differentiation in vitro. *Tissue Eng Pt A* 2009;**15**(6):1427–36.
3. Lim JY, Donahue HJ. Cell sensing and response to micro- and nanostructured surfaces produced by chemical and topographic patterning. *Tissue Eng* 2007;**13**(8):1879–91.
4. Gates BD, Xu Q, Stewart M, Ryan D, Willson CG, Whitesides GM. New approaches to nanofabrication: molding printing, and other techniques. *Chem Rev* 2005;**105**(4):1171–96.
5. Geissler M, Xia Y. Patterning: principles and some new developments. *Adv Mater* 2004;**16**(15):1249–69.
6. Heule M, Vuillemin S, Gauckler LJ. Powder-based ceramic meso- and microscale fabrication processes. *Adv Mater* 2003;**15**(15):1237–45.
7. ten Elshof JE, Khan SU, Göbel OF. Micrometer and nanometer-scale parallel patterning of ceramic and organic–inorganic hybrid materials. *J Eur Ceram Soc* 2010;**30**(7):1555–77.
8. Xia YN, Whitesides GM. Soft lithography. *Annu Rev Mater Sci* 1998;**28**:153–84.
9. Bauer W, Ritzhaupt-Kleissl HJ, Hausselt J. Micropatterning of ceramics by slip pressing. *Ceram Int* 1999;**25**(3):201–5.
10. Fanelli AJ, Silvers RD, Frei WS, Burlew JV, Marsh GB. New aqueous injection molding process for ceramic powders. *J Am Ceram Soc* 1989;**72**(10):1833–6.
11. Knitter R, Bauer W, Göhring D, Haußelt J. Manufacturing of ceramic microcomponents by a rapid prototyping process chain. *Adv Eng Mater* 2001;**3**(1-2):49–54.
12. Piotter V, Gietzelt T, Merz L. Micro powder-injection moulding of metals and ceramics. *Sadhana* 2003;**28**(1):299–306.
13. Holthaus M, Rezwan K. Comparison of three microstructure fabrication methods for bone cell growth studies. *ASME Conf Proc* 2008;**48524**:483–90.
14. Holthaus MG, Kropp M, Treccani L, Lang W, Rezwan K. Versatile crack-free ceramic micropatterns made by a modified molding technique. *J Am Ceram Soc* 2010;**93**(9):2574–8.
15. Berger J, Grosse Holthaus M, Pistillo N, Roch T, Rezwan K, Lasagni AF. Ultraviolet laser interference patterning of hydroxyapatite surfaces. *Appl Surf Sci* 2011;**257**(7):3081–7.